Published in final edited form as:
J Magn Magn Mater. 2009 May ; 321(10): 1440–1445. doi:10.1016/j.jmmm.2009.02.064.

Design, fabrication and demonstration of a magnetophoresis chamber with 25 output fractions

Chris Carr, **Michelle Espy**[a,*], **Pulak Nath**[a], **Sara L. Martin**, **Michael D. Ward**[b], and **John Martin**[c]

[a] Applied Modern Physics, Los Alamos National Laboratory, Los Alamos, NM 87545, USA

[b] Acoustic Cytometry Systems Inc., Los Alamos, NM 87544

[c] B-9, Los Alamos National Laboratory, Los Alamos, NM 87545, USA

Abstract

Our goal is to develop an instrument for parallel and multiplexed bioassay using magnetic labels. Toward this end we are developing a multi-outlet magnetophoresis instrument incorporating a fluidic flow chamber placed inside a magnetic field gradient. Magnetic microparticles are sorted by their magnetic moment for eventual use as biological labels based on magnetic signature.

In this paper we concentrate on developments in our flow chamber fabrication methods that have allowed us to scale the number of sorting channels from 8 to 25. We present data for instrument performance and reproducibility of sorting.

Key terms

Field-flow fractionation; magnetophoresis; magnetic microparticles; magnetic microspheres; laser microfabrication

---

In conventional laser-based flow cytometry the number of distinct biological labels is limited by the availability of different fluorescent dyes. By utilizing variations in the magnetic moment of microparticles, we have the potential to produce orders of magnitude more biological labels for multiplexed *in-vitro* studies. Much research has been carried out on biomolecular labeling and sorting with techniques ranging from electrophoresis [1] to elutriation [2] to fluorescence activated cell scanning/sorting [3] and magnetic sorting based on immunomagnetic labeling [4]. Sorting based on magnetophoresis has also been demonstrated in many forms, see for example [5–10], and it is one approach to this technique that is detailed in this paper.

In our previous work [11] we described our magnetophoresis instrument, including the magnetic microparticles used (both ferromagnetic and superparamagnetic), the magnet quadrupole and the flow chamber design. We analyzed the forces acting on a single microparticle in flow and from this we were able to model their trajectory for various transit times. The modeled and experimental results compared favorably, though the spread in the experimental data highlighted certain hydrodynamic issues that we were forced to address such

*Corresponding author: Michelle A. Espy, Applied Modern Physics, Los Alamos National Laboratory, MS: D-454, Los Alamos, NM 87545, U.S.A. espy@lanl.gov, T: 505 665 6218, F: 505 665 4507.

as reducing the aspect ratio between the sample inlet and the chamber depth and stabilizing the sheath flow. Having eliminated many of the hydrodynamic instabilities, we then were able to re-sort magnetic microparticles with a high degree of reproducibility.

In this paper we report on the design and a new fabrication process for our flow chambers with the number of output channels scaled up to a maximum of 25, limited by the feature size we are able to cut with our existing laser cutter. A key feature of the fabrication process is the simplicity of design and assembly such that we essentially are able to consider the chambers as disposable. As with the 8-channel flow chambers we have sorted and re-sorted populations of magnetic microparticles, though here we only consider superparamagnetic microparticles.

When magnetic microparticles are placed in a magnetic field gradient they experience a force that is proportional to their magnetic moment. The sum of the forces acting on the microsphere leads to the following equations:

$$F_y = m_a \frac{\partial v_y}{\partial t} = -\rho_a V g + \rho_{sheath} V g + 6\pi\eta a (v_{sheath} + v_y) \quad (1)$$

$$F_x = m_a \frac{\partial v_x}{\partial t} = \frac{MVG}{\mu_0} - 6\pi\eta a v_x \quad (2)$$

where v_x and v_y are the microparticle velocity (m s^{-1}) in the x and y direction, respectively (see Figure 1a), m_a is the microparticle mass (kg), $\partial v/\partial t$ is the acceleration (m s^{-2}), ρ_a and ρ_{sheath} are the densities of the microparticle and the sheath fluid, respectively (kg m^3), V is the microparticle volume (m^3), g is the acceleration due to gravity (m s^{-2}), η is the sheath fluid viscosity (kg m^{-1} s^{-1}), and a is the microsphere radius (m). Note that the sheath velocity is assumed to be constant. M is the volume magnetization of the microsphere in A m^2, μ_0 is the free space permeability ($4\pi \times 10^{-7}$ H m^{-1}), and G is the magnetic field gradient (constant for a quadrupole magnet) in T m^{-1}). For ferromagnetic microparticles M is constant, resulting in a linear trajectory. For paramagnetic microparticles, the value of M is a function of the external magnetic field.

This principle can be used to sort magnetic microparticles for use as biological labels in multiplexed assays (as is our goal) [12]. The subsequently magnetically labeled biomolecules could be characterized in flow by their magnetic signature using a sensor such as a Giant Magnetoresistive sensor) (GMR) [13]. Or biomolecules labeled with magnetic microparticles can then be sorted in the same way, with the biomolecule total magnetic moment depending on the number of bound labels and their individual magnetization [14]. Typically magnetophoretic sorting of cells has been binary, but our method demonstrates potential for multiplexed sorting based on magnetic labeling.

Figure 1a shows the force diagram for a single magnetic microparticle flowing through our magnetophoresis instrument. Summing the forces on each microparticle allows us to formulate Equations (1) and (2) and hence model the trajectory [11].

The magnetic separation was based on a quadrupole magnet. This particular design of magnet was chosen to provide a linear field gradient for microparticle sorting. The $SmCo_5$ permanent magnet pieces were 6.25×7×8.5cm while the iron pole pieces were 3.75×8.5×8.5cm. The length of the magnet is 8.5cm; considerably shorter than the overall length of the sorting chamber. The field gradient was measured using a Hall probe and was found to be 17 Tm^{-1} within the bore of the magnet. With the flow chamber positioned in the magnet, the sample inlet tube is

located just far enough off-centre that the microparticle trajectory is essentially only parallel to the x-axis (see Figure 1). We are aware that outside the bore of the magnet the field is non-zero. To reduce the effect of the stray field on the magnetic microparticles while they are still in the sample syringe (i.e. to minimize the possibility of agglomeration), we place a 1mm thick mumetal plate above the magnet to shield the field. The sorting chamber also protrudes below the magnet, thus the microparticle trajectory will again be influenced by the stray field (though to a much lesser extent compared to within the bore of the magnet) as they flow towards the collection bins.

Prior to running experiments to sort magnetic microparticles, we determine the appropriate flow settings by running tests with food coloring as the sample. This allows us to vary the flow through the individual sheath inlets by means of a clamp (note that they are still fed from the same pressure-driven source) such that a non-magnetic sample in the absence of a magnetic field will appear in a pre-chosen collection bin (or bins). The food coloring also allows us to measure the transit time through the magnet. Figure 2a shows a detail of the collection bin region for the 8-channel flow chamber during a pre-test check with food coloring. The sample stream (red food color) is focused and channeled by the dividing walls and goes into bin 2 (with little or no visual evidence of the sample going into bins 1 and 3). The green food color is from one of the sheath supply inlets and shows that there is smooth laminar flow with no turbulent mixing in the chamber.

During each experiment we use 10 μm diameter non-magnetic, latex fluorescent microparticles (Polysciences, Warrington, PA) to ensure that any run-to-run variability is kept to within a few percent. These are counted in the same way as the magnetic microparticles (described below).

A key requirement for magnetic microparticles for use as biological labels for multiplexed assay is that they have a wide range of magnetic moments to provide a wide range of labels. Permanent magnet material such as $SmCo_5$ is an ideal candidate since it has a high remnant magnetization, but this can also cause problems with agglomeration. In general, any ferromagnetic material has to be handled much more carefully than either paramagnetic or superparamagnetic material and sample concentrations have to be typically lower. Previously [11] we have used both commercial ferromagnetic and superparamagnetic microparticles in sorting experiments to validate performance. These were chosen because they were supplied with a known size distribution and had magnetic moments in the range of interest. We have not investigated the variations in magnetic content of these commercial beads but they appear to be quite uniform based on our sorting results. In this paper we have used only 8±0.23 μm diameter superparamagnetic particles (Bangs Laboratories, Fishers, IN). These particles consist of a functionalized polymer impregnated with iron oxide, giving a total density of 1.2g cm^{-3}. The microparticles have a calculated magnetic moment of ~8×10^{-13} Am^2 (the manufacturer-supplied magnetization curve showed a saturation magnetization of 2.54 Am^2 kg^{-1} at ~5×10^4 Am^{-1}).

Typical sample volumes for the experiments were 1–2mL consisting of 0.5mL of magnetic microparticles in solution (concentrations of the order of 10^5–10^6 microparticles/mL) with the remainder being fluorescent microparticles in a solution of de-ionized water and Pluronic™ surfactant (MP Biomedicals, Solon, OH). The Pluronic™ appeared superior to sodium dodecyl sulfate (SDS) (the surfactant we used in previous studies) at preventing agglomeration.

Our experimental sorting method is described elsewhere [11] and described only briefly here. The collection channels on the flow chamber are connected to output collection syringes. The chamber has a differential sheath design, as shown in Figure 1b. The larger sheath stream, “Sheath 1,” is provided by a regulated pressure system. For initial studies, a syringe pump provided “Sheath 2,” but this was later changed to a single pressure system driving both sheath

streams, which greatly improved hydrodynamic stability. The sheath is 0.125% Pluronic™ in distilled water that is passed through a 0.2-μm filter prior to the chamber. Another single syringe pump provides the sample stream, and a multiple syringe pump withdraws the twenty-five outlet streams for the collection bins. We observed that the sheath's stream speed in the chamber (and hence microparticle transit time through the 8.5 cm of the bore of the magnet and deflection) is largely regulated by the speed of the withdrawal syringe pump. The differential sheath design utilizes standard flow cytometry techniques that in principle generate uniform fluid flow through the chamber [3].

On completion of the sort, the contents of each collection bin syringe were transferred to a test-tube, centrifuged to remove excess sheath and subsequently counted using a Caliber™ FACs instrument (Becton Dickinson & Company, Franklin Lakes, NJ). To reduce any potential loss of microspheres at this step, we are in the process of modifying the design so the collection bins are fed directly to the test tubes. The measurement "gates" on the FACs were pre-determined by running a high concentration of microparticles (both magnetic and fluorescent) through the instrument, and these gates were kept constant throughout the counting process. More information can be found in our earlier work [11].

Figure 1b shows a schematic of the 8-channel flow chamber. The external width of the chamber ranges from 35.0 mm (8-channel) to 38.4mm (25-channel) to 41.2 mm (14-channel); this dimension necessarily changes to permit more collection bins (or wider bins) to be added. The external length of the chamber is kept constant at 173 mm, while the external thickness is approximately 3.8mm for all. The internal dimensions of the chamber range from a width of 18.7mm (8-channel) to 26.6mm (14–25 channel), while all have a depth of 0.8mm. The chamber dimensions take into account various parameters including magnet dimensions, microparticle diameter, number of discrete populations required and fabrication processes.

There are three inlets at the top of the chamber: one for the sample and two for the sheath supply. The sample inlet tube is a 362 μm OD, 248 μm ID polyimide-coated glass capillary (Polymicro Technologies, Phoenix, AZ) though for added mechanical durability, it is glued inside a piece of 750 μm OD, 500 μm ID PEEK™ tubing (Upchurch Scientific, Oak Harbor, WA). The sample is supplied from a 3 mL plastic syringe using a single syringe drive (Harvard Apparatus, Holliston, MA). Each sheath supply is connected via Silastic™ tubing (Dow Corning, Midland, MI) to the same pressure-driven supply. The sheath is a solution of 0.125% (by weight) Pluronic™ and de-ionized water and it passes through a 0.2 μm membrane filter prior to entering the flow chamber. One of the problems associated with the chamber design is the occurrence of small air bubbles collecting at the sheath inlets that affect the hydrodynamic flow. To alleviate this, each sheath inlet has a "bleed off" valve connected to it (with both the inlet itself and the valve made from PEEK™ tubing). At the end of the collection channels, a piece of PEEK™ tubing glued into the chamber is connected to a piece of Silastic™ tubing for sample collection.

At the other end of the flow chamber, below the collection bins are the extraction syringes. In our experience, having the outlet tubes merely drain into collection vials led to problems with reproducibility. The syringe drives (KD Scientific, Holliston, MA) are specifically designed for multiple syringes and have been modified to take up to 20 syringes per drive. At present we run them with at most 13 in any one drive. If we are successful at modifying the set-up to draw directly into test tubes, this extraction protocol may be simplified. Figure 2b shows the experimental set up.

Since the critical flow chamber dimensions are sub-mm, using a standard milling machine is not a reliable option for chamber construction. In our lab we have access to a CO_2 laser cutter (M360, Universal Laser Systems, Scottsdale, AZ) that allow us to fabricate chambers with a

minimum feature dimension of ~100 μm. Figure 3a and 3b shows a detail of the design for the inlet and outlet regions of the middle layer of the flow chamber.

The chambers were fabricated using double sided tapes (ACcare® 8570, Adhesive Research Inc., Glenrock, PA) and a three sets of Acrylic sheets (top layer, middle layer, and bottom layer). The tape is first applied on both sides of a 0.5 mm thick acrylic sheet. One side of the double sided tape has a protective film which is not removed during this process. The laser cutter is then utilized to cut the acrylic sheet and the double sided tapes according to the channel layout. The power and the writing speed of the laser cutter is optimized such that the acrylic sheet/double sided tape assembly is cut all the way with out excessive burning. A second sheet of Acrylic (1.5 mm thick, Optix® acrylic sheet, Paskolite Inc, Columbus, Ohio) is then utilized to obtain the top and bottom plate for the fabrication of the enclosed chamber. The same CO_2 laser cutter is utilized to cut out acrylic pieces from the bulk sheet. The top plate is cut such that it has through holes to form inlets and outlets connections. For a 25 channel output design, special optimization of the laser cutter power and speed was required so that 25 through holes can be fit into the width of the channel. The acrylic section with the double sided tapes is then used as the middle layer. The enclosed chamber is formed by removing the protective films and sandwiching this layer with the top and bottom acrylic. The top layer is aligned with the bottom middle layer such that the inlet and outlet holes are aligned with the channel layout. A special clamping mechanism is utilized to apply uniform pressure throughout the stack for improved bonding by the double sided tapes. Chambers fabricated this way with all layers having the same width were found to be moderately robust and able to flow at chamber pressures up to ~2 psi. However we observed this was not adequate for the reliable performance at the highest of our flow rates. In order to obtain higher bonding strength, the top and bottom plates were cut slightly bigger (~1–2 mm on all four sides). This design allowed us to obtain additional space between the bottom and the top plates throughout the perimeter of the channel. This space was then filled up with epoxy cement (Loctite Marine Epoxy, Hankel Consumer Adhesives Inc., Avon, OH) and cured for about 2–4 hours. The epoxy allowed additional strength to the bonding and the chamber was able to withstand flow at chamber pressures up to ~15 psi. A step by step schematic diagram showing the cross section of the channel at different fabrication steps is presented in Figure 4.

In the next year we are planning to scale up the number of sorting bins further, with the goal of achieving 50 outlet channels. This will require the use of a laser cutter capable creating of smaller features in the flow chamber (our present device is limited to features ~100 μm in width). An Excimer laser based microfabrication tool available at the Los Alamos Center for Integrated Nanotechnologies will be utilized. Such a device has the ability to obtain features as small as 5 μm. This laser cutter could be utilized to obtain channels containing up to 100 outlets within the limited width of the channel.

The chamber fabrication process we have described is flexible and allows easily for changes in chamber dimensions and number of outlet bins. The most time consuming step of our chamber manufacturing process is gluing the inlet and outlet PEEK™ tubing. Several chambers can be cut and fabricated at one time such that the devices can be essentially considered disposable.

To determine the flow chamber performance we sorted the 8 μm diameter superparamagnetic microspheres described above. Because of the size and magnetic monodisperse properties of the microspheres, we expect these microspheres to (under ideal conditions) all sort to a single bin, with the deflection proportional to the moment (which doesn't change) and the transit time in the magnet, which we can vary. We then collected populations from selected outlet bins, and re-sorted that material under the same conditions. The reproducibility of sorting (i.e.

microspheres from bin “A” returning to bin “A”) can thus be characterized. Figure 5 shows two sets of data for sorting (a) and resorting (b) in our chambers.

The 8-channel chamber data (left) were sorted at a 0.25 ml/min-channel flow rate corresponding to a transit time through the magnet of ~ 40 sec. The fluorescent (non-magnetic) microspheres which were flowed as controls (data not shown) arrived in collection bin #2, while the magnetic microspheres are observed to be collected primarily in bin #5. As one would expect, our experiments indicate increasing deflection with transit time or magnetic moment of the particles. In preliminary 8-channel chamber designs we also observed an increasing spread in the distribution of microparticles [11] as the transit time increased. The origin of this effect was ruled out as being from microparticle diffusion and variations in magnetic content. We ascertained that the dominant source of this spread was hydrodynamic in origin and alterations to the sheath supply method and also to the dimensions of the sample inlet tube made the distribution much sharper [11]. Some of these hydrodynamic effects had to do with the microparticles experiencing different flow velocities due to a spread in the sample stream, which was partially solved by changing the aspect ratio of the inlet tube and chamber thickness [11]. As shown in Figure 2 with food coloring, and determined by our non-magnetic microspheres, it appears that the sample stream is narrow (i.e. within one bin), however these tests do not rule out a broadening of the sample stream in the magnetic microspheres which could be caused by agglomeration or other interactions.

The data at right in Figure 5 are from a 25-outlet chamber at a flow rate of 0.2 ml/min-channel corresponding to a transit time through the magnet of ~16 sec. Sorting experiments in the 25-channel chamber indicate the same features of increasing deflection with transit time. In this chamber the fluorescent beads (not shown) primarily land in bin #7. The 25 channel data shown in Figure 5 indicate that we are still somewhat limited by hydrodynamic spread in the sample stream. For the 8-channel chamber bin #5 was resorted and here 89% of the microparticles that originally ended up in bin 5 return to the same bin when re-sorted. For an extraction rate of 0.4mL/min, the initial peak is in bin 3 and 84% of those microparticles return to bin 3 (data not shown). More data on the performance of the 8-channel chamber is presented in [11]. For the 25-channel chamber we observed both in the sort and re-sort data that 85% of the microspheres re-sort over three bins. The 25 chamber data shown was obtained in a flow-chamber fabricated prior to shifting the method of adding epoxy around the bonded channels (see right side of Figure 4), which were only able to withstand about 2 psi pressure. We have qualitatively observed that those previous chamber designs often were not as hydrodynamically stable as the new chamber design appears to be (likely due to sheath seeping into the side walls) while flowing. Tests with the new chambers are underway and we are optimistic that with the appropriate chamber design we will be able to continue to narrow our collection capabilities to a single bin for monodisperse microspheres.

The ultimate aim of the work is described here is to produce reproducible populations of microspheres sorted by their magnetic moment for use in multiplexed bioassay. Rather than binary (magnetic or not) methods, we have demonstrated that it is possible to build chambers capable of reliable sorting of a continuum of magnetic moments. Such applications could be multiplexed assay such as we attain [13], collection of immunomagnetically labeled cells [14], or precise control of microspheres for manipulation in flow [15], or others. We have demonstrated that with relatively simple fabrication methods and flow-chamber design, magnetophoresis with up to 25 unique populations is possible.

Acknowledgments

This work was funded by the US NIH under Grant RR019626-01. The authors also acknowledge the support of the National Flow Cytometry Resource and Los Alamos National Laboratory under NIH Grant RR-01315. The authors wish to thank Christina Hanson, Henrik Sandin, Yonathan Araya, and John Gomez for their assistance.

References

1. Schütt, W.; Klinkmann, H., editors. Cell Electrophoresis. Berlin: Walter de Gruyter; 1985.
2. Bauer J. J Chromatogr B 1999;722:55.
3. Shapiro, HM. Practical Flow Cytometry. New York: Wiley-Liss; 1995.
4. Thiel A, Scheffold A, Radbruch A. Immunotechnol 1998;4:89–96.
5. Chalmers JJ, Zborowski MJ, Sun LP, Moore L. Biotechnol Progr 1998;14:141.
6. Moore LR, Zborowski M, Sun L, Chalmers JJ. J Biochem Biophys Meth 1998;37:11. [PubMed: 9825297]
7. Sun LP, Zborowski M, Moore LR, Chalmers JJ. Cytometry 1998;33:469. [PubMed: 9845442]
8. Latham AH, Freitas RS, Schiffer P, Williams ME. Anal Chem 2005;77:5055. [PubMed: 16053322]
9. Carpino F, Moore LR, Zborowski M, et al. J Magn Magn Mater 2005;293:546.
10. Pamme N, Manz A. Anal Chem 2004;76:7250. [PubMed: 15595866]
11. Espy MA, et al. Cytometry Part A 2006;69A:1132.
12. Sandin H, Carr C, Matlachov AN, et al. Int Congress Series June;2007 1300:271.
13. Carr C, Matlachov AN, Sandin H, et al. IEEE Trans Appl Supercond 2007;17(1):808.
14. Schneider T, Moore LR, Jing Y, et al. J Biochem Biophys Methods 2006;68:1. [PubMed: 16675023]
15. Pamme, N., et al. Magnetic microparticles as maneuverable solid supports for multistep (bio)reactions in continuous flow; presented at the Magnetic Carriers Conference; May 22–24, 2008; Vancouver, BC.

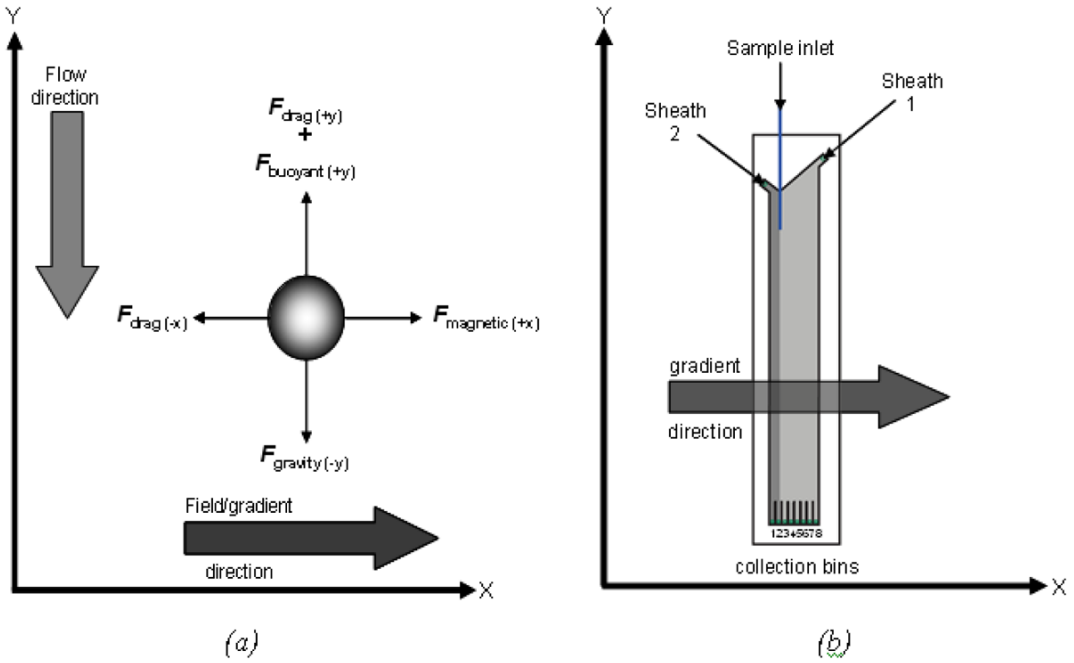

Figure 1.
(a) Force diagram for a magnetic microparticle in flow; (b) Schematic diagram of the flow chamber

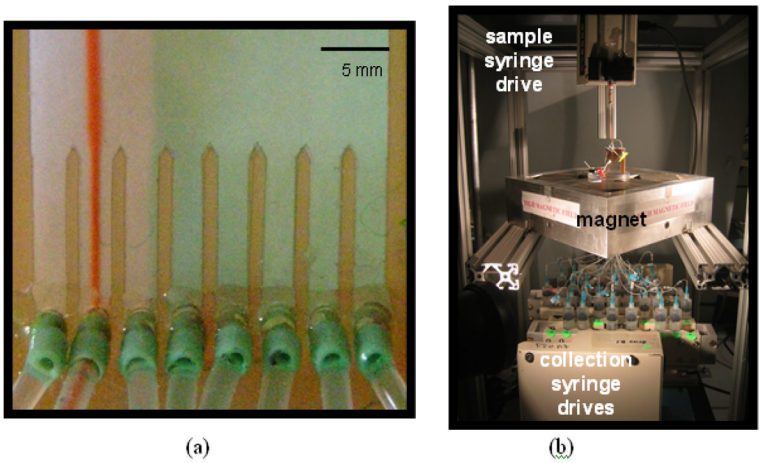

Figure 2.
(a) flow characterization for the 8-channel flow chamber using food coloring dyes; (b) Experimental setup showing the magnet quadrupole and the sample/extraction syringes.

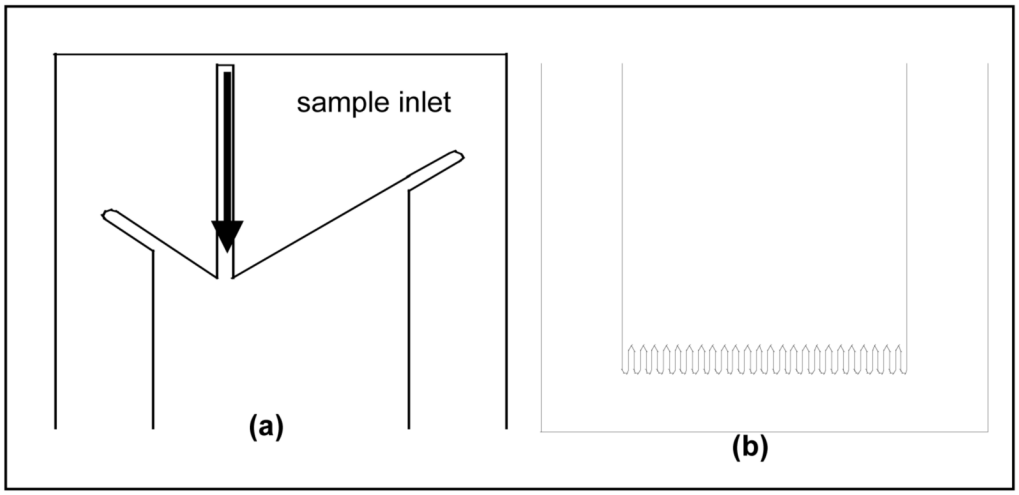

Figure 3.
Schematic of the flow chamber design (a) inlet of the middle layer; (b) outlet of the middle layer

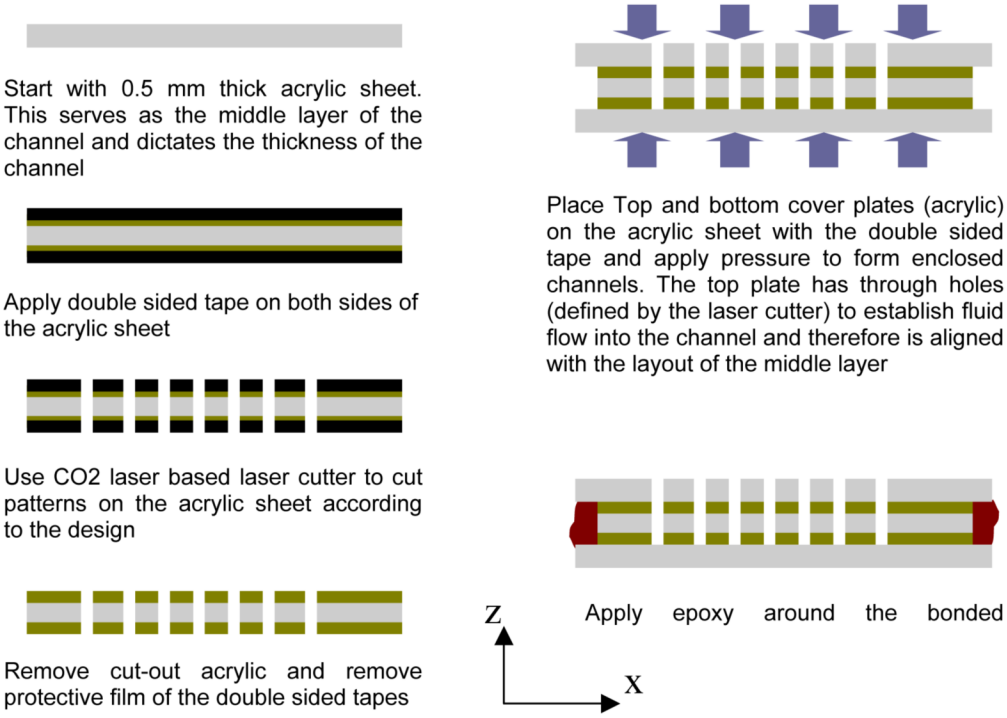

Figure 4.
Schematic cross-section showing different steps of the fabrication process

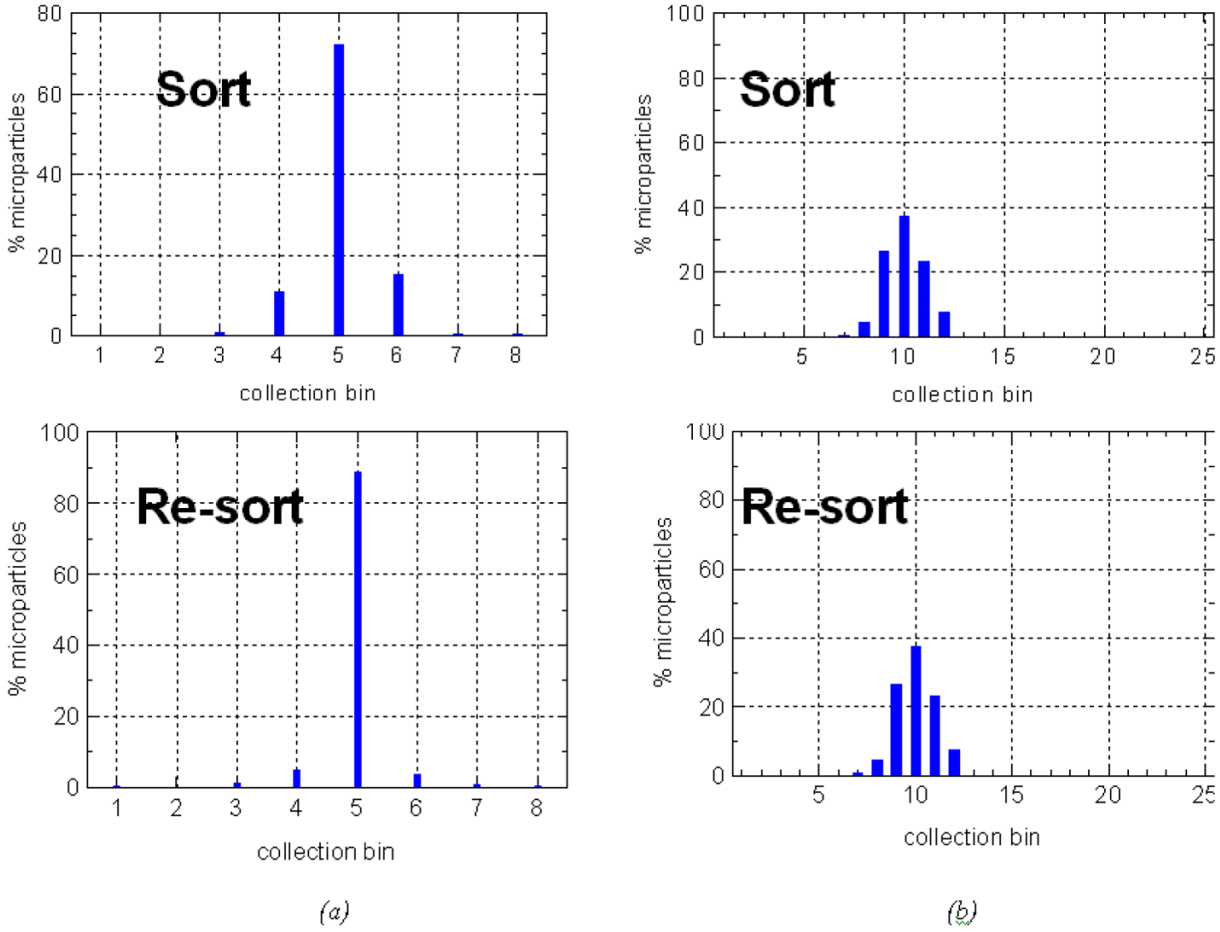

Figure 5.
Data from the initial sort and re-sort (a) 8-channel and (b) 25-channel flow chambers.